Science and Technology Indonesia
e-ISSN:2580-4391 *p*-ISSN:2580-4405
Vol. 11, No. 3, July 2026

Research Paper

Nano-Enhanced Tri-Organotin (IV) Complexes from a Ciprofloxacin Hybrid: Synthesis, Characterization, and Superior Antifungal Activity

Aliyaa Dhahir Mohsin[1*], Angham G. Hadi[1], Rana A. K. Al-Refaia[1]

[1]*Department of Chemistry, College of Science, University of Babylon, Babylon, 51002, Iraq*
***Corresponding author**: sci139.alaa.dahar@uobabylon.edu.iq*

Abstract
Organotin (IV) compounds are of significant interest in both the chemical and medicinal sectors. Among these, tri-organotin (IV) derivatives (R3SnX) stand out due to their potent biological activity and their distorted trigonal bipyramidal geometry. The present study details the synthesis, nano-formulation, and improved antifungal activity of three new tri-organotin (IV) complexes. These complexes have been synthesized from a hybrid ligand, formed from ciprofloxacin and 5-aminosalicylic acid, followed by modification of the carboxylate functional group with chloroacetic acid. These compounds have been completely characterized by FT-IR, multinuclear NMR spectroscopy (^{1}H, ^{13}C, ^{119}Sn), and CHNS analysis. To enhance their biological activity, the synthesized complexes have been nano-formulated with triangular silver nanoparticles (AgTNPs). The antifungal activity of both pure and nano-formulated complexes has been investigated against *Fusarium spp*. In vitro antifungal assays against *Fusarium spp*. revealed that the triphenyltin complex (T3) was the most active among the pure compounds, achieving a 20% inhibition rate at 2 mg/mL, attributed to its high lipophilicity and aromatic content. Remarkably, the nano-formulated version (AgTNPs-T3) demonstrated a significant synergistic effect, increasing the inhibition rate to 55% at the same concentration, a 2.75-fold enhancement compared to the unmodified complex. This superior performance is attributed to the high surface area-to-volume ratio and sharp vertices of the AgTNPs, which facilitate better membrane penetration and ROS generation.

Keywords
Tri-Organotin (IV) Complexes, Triangular Silver Nanoparticles, Nanocarrier, Antifungal Activity

Received: 2 February 2026, Accepted: 26 April 2026
https://doi.org/10.26554/sti.2026.11.3.982-993

1. INTRODUCTION

Organotin (IV) compounds are significant in the formation of structural motifs characterized by various coordination geometries and forms due to their unique structural properties (Joshi et al., 2020). With the increasing incidence of fungal infections and the emergence of resistant strains, there is an urgent need for the continuous development of new, more potent antifungal agents (Nopitasari et al., 2021 Arraq and Hadi, 2022). In this regard, organotin (IV) compounds with at least one direct Sn−C bond are recognized as an important class of active organometallic compounds. Also, they are of great interest to the chemical and medicinal sectors (Al-Shemary et al., 2024; Erfan et al., 2024). The various applications of organotin complexes have attracted the attention of researchers worldwide in recent decades. Among these, tri-organotin (IV) compounds possess more potent biological activity than their mono- and di-organotin counterparts, which is often related to the optimization of their lipophilicity and geometry (Li et al., 2025; Dias et al., 2015). These compounds possess substantial potential as anticancer, antibacterial, and antifungal agents (Al-Shemary et al., 2024). Currently, nanotechnology has greatly influenced drug development by enabling innovative approaches to overcome challenges faced by conventional drugs, including low solubility, low bioavailability, and poor targeting. As a rapidly advancing interdisciplinary domain, nanotechnology integrates principles from chemistry, physics, and biology to engineer innovative nanomaterials. These nanoparticles are particles with at least one dimension measuring between 1 and 100 nanometers. Nanotechnology encompasses the production, characterization, and uses of various nanoparticles. Noble metals, including gold, silver, and platinum, are commonly used to produce nanoparticles via various chemical and physical methods (Joshi et al., 2020; Hano and Abbasi, 2022; Radulescu et al., 2023; Al-Refaia et al., 2024; Soleimani et al., 2022; Fithri et al., 2025; Raji and Bader, 2024). On the other hand, several forms of organic and inorganic nanoparticles have been developed, especially metal and metal oxide nanoparticles, because they have various modes of action (Al-Refaia et al.,

2019; Saputra et al., 2024). For example, metallic nanoparticles, such as silver nanoparticles (AgNPs), have been studied not only for their antimicrobial potential but also for their potential as drug delivery systems. This is because of their large surface area-to-volume ratio, enabling efficient drug delivery (Preethi et al., 2024; Chandrakala et al., 2022; Polinarski et al., 2021). Furthermore, triangular silver nanoparticles (AgTNPs) have been shown to exhibit greater potential than spherical nanoparticles due to shape-dependent properties, such as increased surface reactivity, thereby displaying greater biological activity (Yin et al., 2022). Furthermore, the increased antibacterial efficacy of AgTNPs compared to spherical nanoparticles is attributed to their shape, sharp edges, and vertices, which facilitate improved adhesion and penetration into the cell membrane, therefore leading to bacterial death (Rodriguez Barroso et al., 2023). A strategy for developing synergistically effective next-generation antifungal agents combines the intrinsic bioactivity of organometallic compounds with the benefits of nanocarrier delivery systems. By encapsulating bioactive agents on nanocarriers such as AgTNPs, their bioavailability can be improved and, most importantly, their bio-efficacy enhanced (Han et al., 2024). In agreement with the above-mentioned basis, the present scientific work is dedicated to the design and evaluation of a new series of hybrid antifungal compounds using a Schiff base ligand based on the antibiotic ciprofloxacin and 5-aminosalicylic acid, and then modified. In order to harness the advantages of nanotechnology, the synthesized compounds were loaded onto triangular silver nanoparticles (AgTNPs) using green synthesis methods. This work evaluates the in vitro antifungal efficacy of the synthesized compounds against *Fusarium spp*. and compares the efficacy of these compounds with their AgTNPs-loaded forms. The present work aims to establish the efficacy of AgTNPs as a tool for boosting the antifungal efficacy of tri-organotin (IV) complexes.

2. EXPERIMENTAL SECTION

2.1 Materials and Instrumentation

The compounds utilized in this work were of the highest quality and required no additional purification. Methanol, ciprofloxacin, thionyl chloride, 5-aminosalicylic acid, chloroacetic acid, trimethyltin chloride, tri-butyltin chloride, and tri-phenyltin chloride were purchased from Sigma-Aldrich. UV-Vis absorption spectra were obtained using T80 UV-VIS Spectrometer PG Instruments Lt, Scanning electron microscope (SEM), Fourier transform infrared (FT-IR) analysis, Nuclear magnetic resonance (^{1}H, ^{13}C, ^{119}Sn), and Elemental analysis.

2.2 Methods

2.2.1 Synthesis of Triangular Silver Nanoparticles (AgTNPs)

Triangular silver nanoparticles have been prepared in previous work (Mohsin et al., 2026). Briefly, garden cress extract was prepared by soaking 20 g of washed, air-dried seeds in 100 mL deionized water for 24 h, then heating at 100 °C for 35 min, filtering, and storing at 4 °C. After that, silver seeds were synthesized by mixing 20 mL aqueous $AgNO_3$ (2.9-10.4 M) with 40 mL plant extract in an ice bath, followed by the dropwise addition of 0.6 mL NaOH (0.1 M) under vigorous stirring; the resulting yellow solution was aged in the dark for 2 h. Finally, silver nanosheets were produced by combining 5 mL of the prepared seeds with 6 mL trisodium citrate, 6 mL of a Chitosan/Gelatin blend (1:1, 0.70 mM), and 240 μL H_2O_2 (30% w/w) in 150 mL deionized water. The mixture was stirred for 50 min at room temperature, where the emergence of red, green, and blue hues confirmed successful silver nanosheet synthesis.

2.2.2 Synthesis of Ciprofloxacin 5-Aminosalicylic Acid (CAS)

Based on previous research by (Abed-Al Zahra and Hadi, 2025). Stoichiometric amounts of ciprofloxacin (3.313 g, 10 mmol) and 5-aminosalicylic acid (1.53 g, 10 mmol) were reacted via condensation to yield the ligand (CAS) (by first converting the carboxylic group in ciprofloxacin to an acyl group by $SOCl_2$, followed by a reaction with 5-aminosalicylic acid). The precursors were dissolved in 30 mL of methanol and refluxed for 4 h. The resulting white precipitate was filtered, dried, and fully characterized, as shown in Figure 1. The ligand (CAS): white precipitate, yield: (90%), m.p: 316.0-317.2 °C, and elemental analysis % calculated (Found): C: 61.62 (60.34), H: 5.48 (4.97), and N: 12.68 (12.04).

2.2.3 Synthesis of Tri-Organotin (IV) Complexes

According to the procedure described by Arraq and Hadi (2022). These complexes were prepared by using a 1:1 molar ratio (metal: ligand). Appropriate amounts of Me_3SnCl (0.6 g: 1.41 g), Bu_3SnCl (0.976 g: 1.41 g), and Ph_3SnCl (1.156 g: 1.41 g) were each dissolved in 30 mL of methanol. The solutions were stirred for 10 min at 50 °C, then refluxed for 5 h. The resulting precipitates were filtered and dried. Subsequently, each tri-organotin (IV) complex was reacted with chloroacetic acid in a 1:1 ratio in methanol, heated, and stirred for 30 min. The final products were filtered, dried, and fully characterized, as presented in Figure 2. T1: white precipitate, yield: 91%, m.p: 324.0–326.1 °C. Elemental analysis % calculated (Found): C, 61.62 (60.34); H, 5.48 (4.97); N, 12.68 (12.04); Sn, 17.27 (16.51). T2: white precipitate, yield: 90%, m.p: 327.1–329.5 °C. Elemental analysis % calculated (Found): C, 56.10 (55.66); H, 6.32 (5.52); N, 6.89 (6.11); Sn, 14.59 (14.03). T3: white precipitate, yield: 92%, m.p: 319.0–321.3 °C. Elemental analysis % calculated (Found): C, 60.50 (59.13); H, 4.50 (3.67); N, 6.41 (6.04); Sn, 13.59 (12.92).

2.2.4 Modification of AgTNPs with Tri-Organotin (IV) Complexes (T1-T3)

According to the procedure described by (Qiao et al., 2023).The interaction between AgTNPs and tri-organotin (IV) complexes (T1–T3) was studied in the presence of NaCl. Briefly, 200 μL of AgTNPs were added to a centrifuge tube, followed by the addition of tri-organotin complexes: T1 (0.020 g, 0.029 mmol),

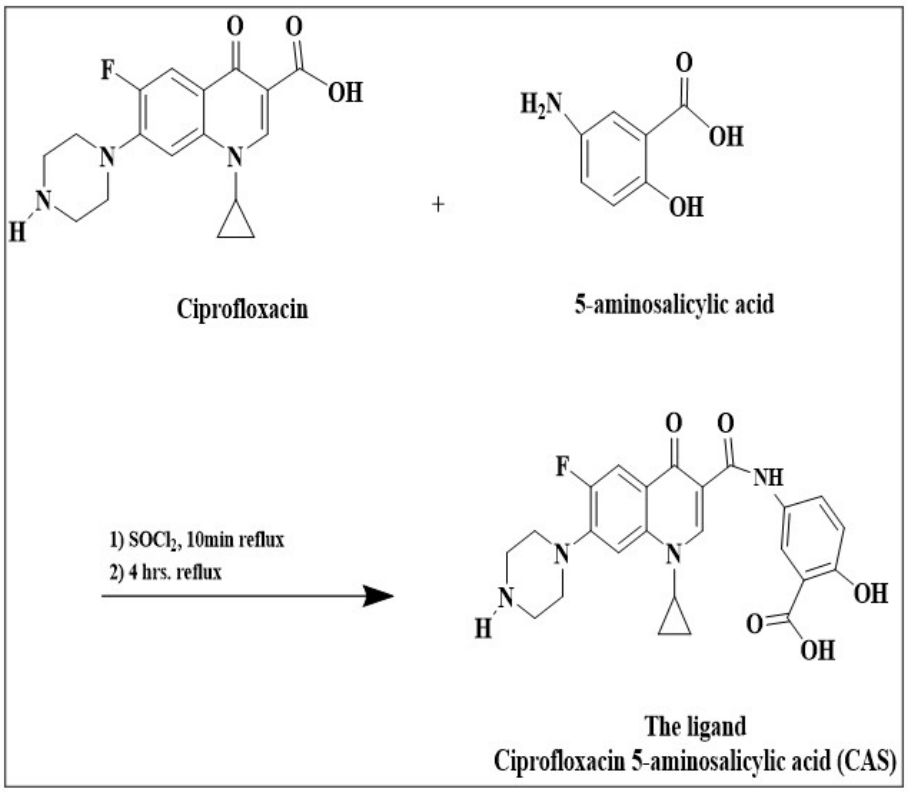

Figure 1. Synthesis of Ciprofloxacin 5-Aminosalicylic Acid (CAS)

Table 1. Physical Analysis Data of the Ligand (CAS) and Its Complexes

Compounds	R	The Color	Melting Point (°C)	Yield (%)	Elemental Analysis % Calculated (Found)			
					C	H	N	Sn
The Ligand (CAS)	-	White	316.0-317.2	90	61.62 (60.34)	5.48 (4.97)	12.68 (12.04)	-
T1	Me	White	324.0-326.1	91	50.68 (49.87)	4.84 (3.65)	8.15 (7.89)	17.27 (16.51)
T2	Bu	White	327.1-329.5	90	56.10 (55.66)	6.32 (5.52)	6.89 (6.11)	14.59 (14.03)
T3	Ph	White	319.0-321.3	92	60.50 (59.13)	4.50 (3.67)	6.41 (6.04)	13.59 (12.92)

T2 (0.024 g, 0.029 mmol), or T3 (0.026 g, 0.029 mmol) to reach a final concentration of 30 μM. Subsequently, 0.05 mL of NaCl solution (4.00 mM) was added and thoroughly mixed. The reaction mixture was stirred for 7 min at ambient temperature. The color change in the reaction tubes was visually inspected, and the absorption spectra in the 500-600 nm range were recorded using a UV-Vis spectrophotometer, as shown in Figure 3.

2.2.5 Assessment of Antifungal Assay

The antifungal activity of tri-organotin (IV) complexes (T1–T3), with and without AgTNPs modification, was evaluated against *Fusarium spp*. isolates from cucumber using the agar dilution method. The agar medium was supplemented with different concentrations (1 and 2 mg/mL) of the complexes. A 1 cm diameter disc, containing mycelial growth from a 6-day-old fungal culture, was placed at the center of each plate. The inoculated plates were then incubated at 25 °C. Treatment efficacy was assessed after 7 days by measuring the radial growth of the fungal colonies (Ali et al., 2025). The inhibition rate was calculated using Equation (1):

$$\text{Inhibition rate (\%)} = \frac{R - r}{R} \quad (1)$$

Where (R) represents the radial growth of the fungal hy-

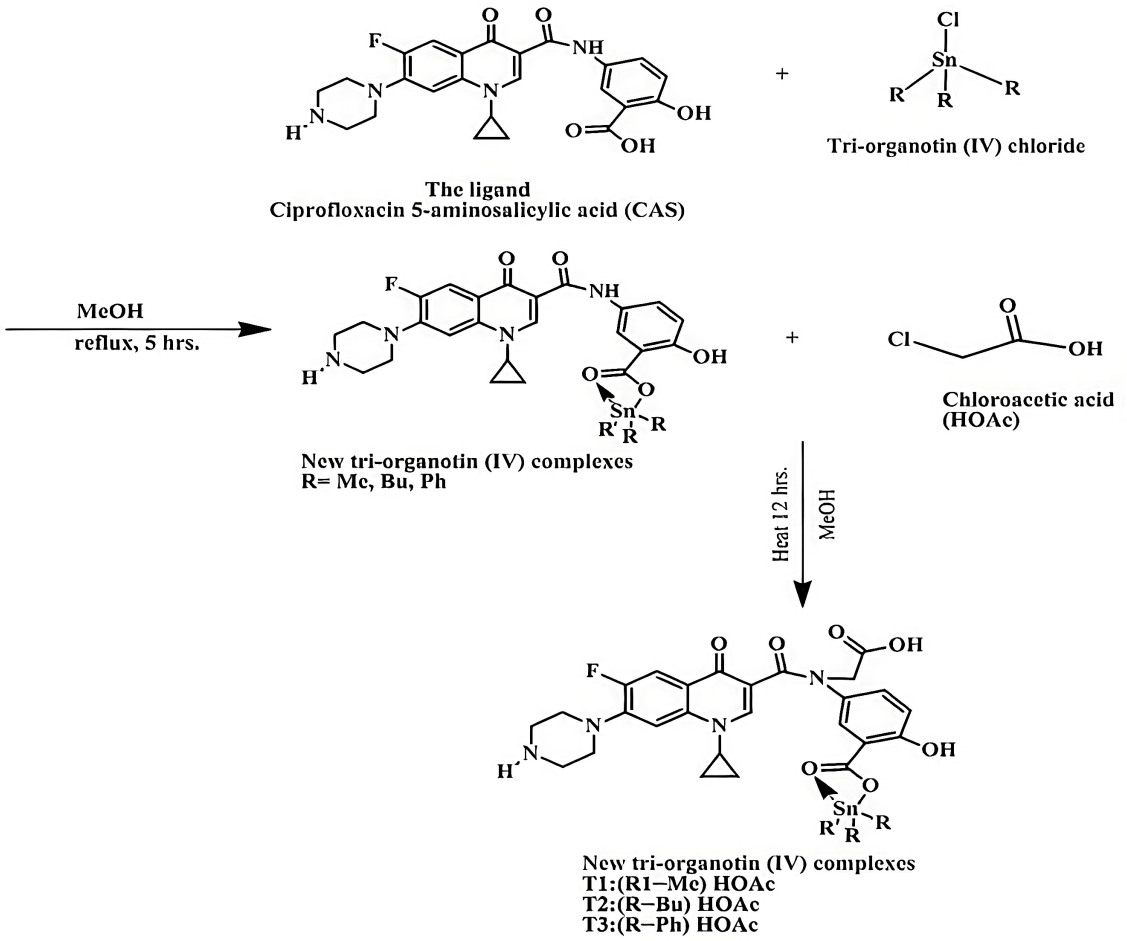

Figure 2. Synthesis of Tri-Organotin (IV) Complexes After Modification with Chloroacetic Acid

phae in the control plate, and (*r*) is the radial growth in the plates treated with the tri-organotin (IV) complexes (T1–T3), with or without AgTNPs modification.

3. RESULTS AND DISCUSSIONS

Three new tri-organotin (IV) complexes (T1–T3) were synthesized by refluxing tri-organotin (IV) chlorides (Me_3SnCl, Bu_3SnCl, and Ph_3SnCl) with a ciprofloxacin 5-aminosalicylic acid ligand, following modification with chloroacetic acid. This procedure follows a substitution reaction mechanism, as illustrated in Figures 1 and 2. Table 1 summarizes the analytical data, including the elemental percentages (C, H, N, and Sn), physical appearance (colors), and melting points of the synthesized complexes.

3.1 FT-IR Spectrum

The FT-IR spectra of the ligand and its complexes (T1-T3) were recorded in the wavenumber range of 4000–400 cm^{-1}, as shown in Figure 4. A significant shift in the broad bands associated with the ligand's carboxyl group was observed upon complexation with tin. This indicates coordination between the ligand and the tri-organotin (IV) compounds via deprotonation of the carboxyl group. Further evidence of coordination is provided by the emergence of new bands assigned to (Sn−C) and (Sn−O) at 570-569 cm^{-1} and 499-487 cm^{-1}, respectively. These bands confirm the linkage between the tin core and the respective aryl, alkyl, or carboxyl groups. These values are in excellent agreement with literature reported for tri-organotin (IV) derivatives, further validating the successful coordination (Arraq and Hadi, 2022). The asymmetric and symmetric vibrations of the carbonyl group were observed at 1627 cm^{-1} and 1625 cm^{-1}, respectively. The differential between theC=O asymmetric and C=O symmetric vibration frequencies (δv) ranged from 168 to 175 cm^{-1}. Minor variations in the frequency suggest chelation or bridging of the carboxylate group, thus confirming a bidentate chelating mode rather than a monodentate coordination. The carboxyl group is associated with the infrared spectrum data for the broad band 2400-3500 cm^{-1} because complexation has caused these groups to shift (Hadi et al., 2021). AgTNPs were characterized in a previous research (Mohsin et al., 2026). While FTIR spectra for complexes after modification with AgTNPs showed slight shifts and intensity changes in the characteristic peaks in the range of 3000-3400

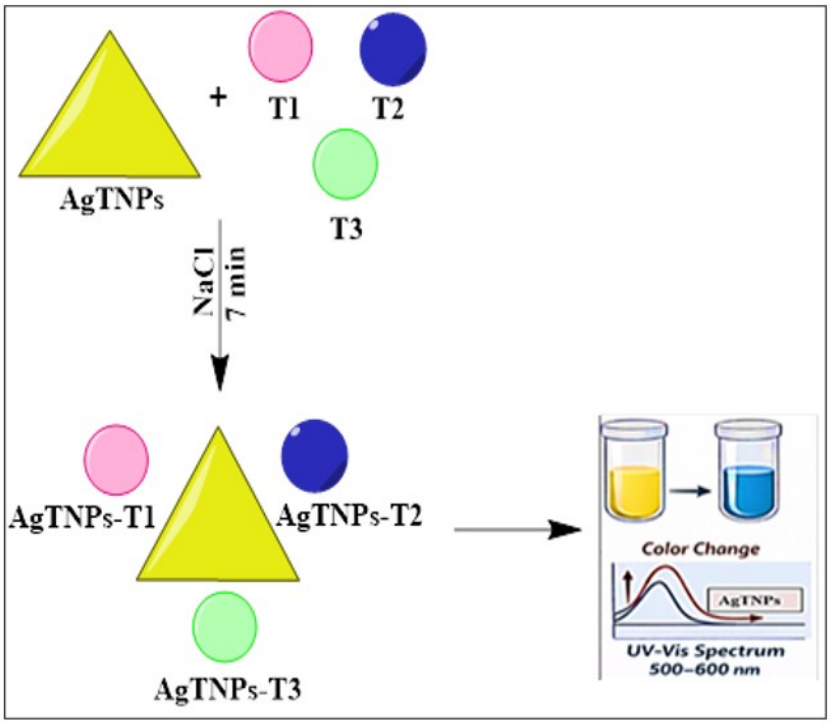

Figure 3. Modification of AgTNPs with Tri-Organotin (IV) Complexes (T1-T3)

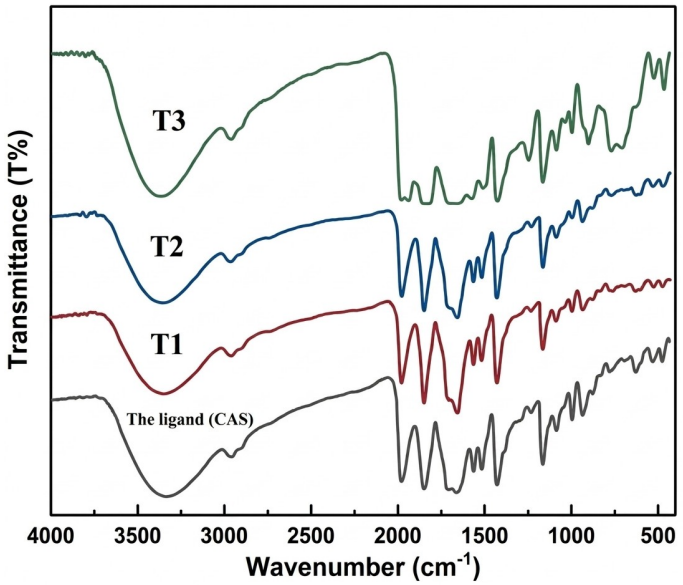

Figure 4. FT-IR Spectra for the Ligand and Tri-Organotin (IV) Complexes (T1-T3)

cm^{-1} of OH stretching from carboxylic acids, and peaks at 1700 cm^{-1}-1200 cm^{-1} corresponded to C=O. Crucially, the persistence of the Sn−C and Sn−O bands confirms that the structural integrity of the organotin complexes remains intact after integration with the AgTNP, as shown in Figure 5. These minor shifts likely arise from non-covalent interactions (such as hydrogen bonding or van der Waals forces) between the complex functional groups and the silver nanoparticle surface (Ali et al., 2025).

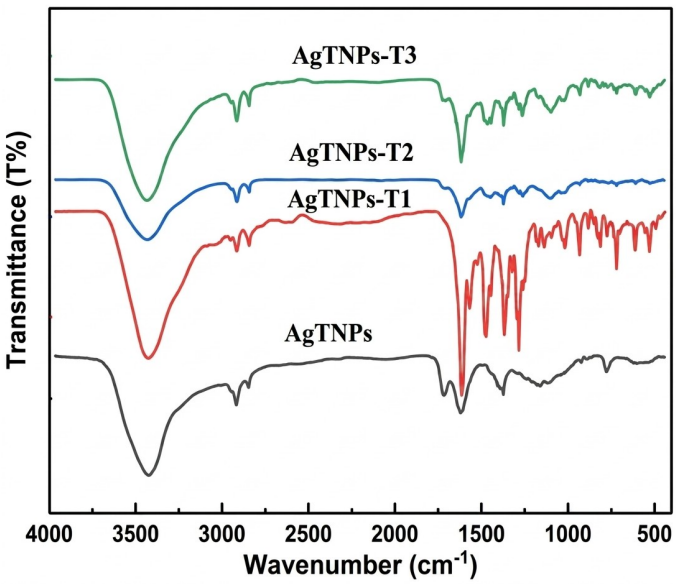

Figure 5. FT-IR Spectra for AgTNPs and Tri-Organotin (IV) Complexes After Modification with AgTNPs

Table 2. The ^{1}H-Nmr Spectra of the Ligand (CAS) and Its Complexes (T1-T3) (Dmso-D6)

Compounds	^{1}H-Nmr
Ligand (Cas)	15.1-14.965 (COOH), 9.6-9.4 (s, 1H, NH), 8.686-7.0 (s, 1H, Ar−H), 4.011 (m, 5H, -Cyclopropyl), 3.779-3.169 (m, 4H, $-N-CH_2-CH_2-N$), 2.891-2.273 (m, 4H, CH_2-CH_2).
T1	9.440 (s, 2H, $_2$NH), 7.967-7.937 (m, 3H, Ar), 7.608 (m, 3H, Ar), 0.857 (s, 9H, $_2$Me), 3.867-3.170 (m, 4H, CH_2-CH_2), 4.127 (m, 4H, Cyclopropane-N).
T2	15.232-15.072 (s, 1H, Alcohol), 9.736-9.599 (s, 2H, $_2$NH), 8.687-7.941 (m, 3H, Ar), 7.623 (m, 3H, Ar), 0.858 (s, 9H, $_2$Me), 4.127 (m, 4H, Cyclopropane-N), 3.971-3.170 (m, 4H, CH_2-CH_2).
T3	9.910-9.658 (s, 2H, $_2$NH), 8.654-7.889 (m, 3H, Ar), 7.603-7.608 (m, 3H, Ar), 2.729 (3H, CH_2), 3.550 (2H, CH_2), 4.223 (4H, Cyclopropane-N), 7.590 (m, 5H, Ar).

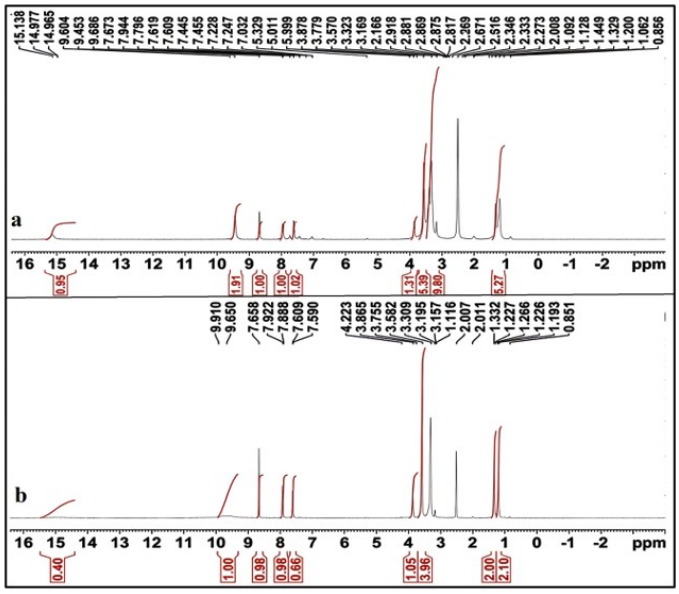

Figure 6. ^{1}H-NMR Spectra of: (a) The Ligand (CAS), (b) Complex T3

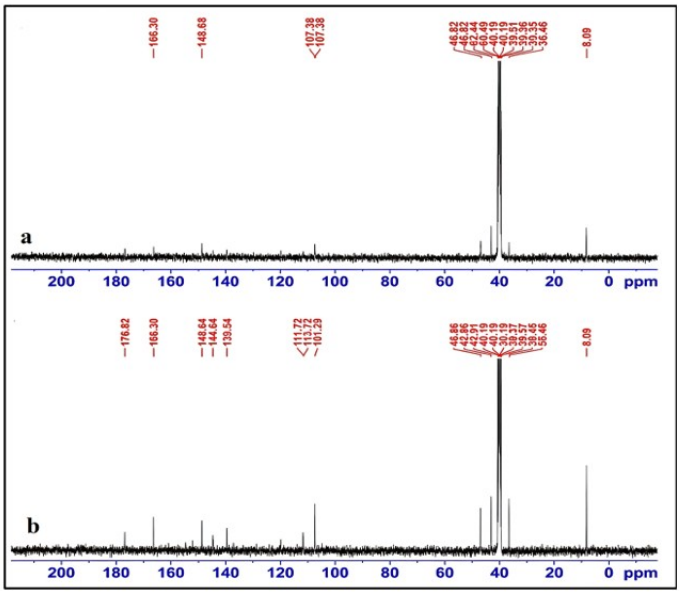

Figure 7. ^{13}C-NMR Spectra of: (a) The Ligand (CAS), (b) Complex T3

3.2 NMR Spectroscopy

The ^{1}H-NMR spectra of the ligand (CAS) and its tri-organotin (IV) complexes (T1–T3), as presented in Table 2, showed the absence of the carboxylic proton (–COOH) signal, which appeared as a singlet at 15.1 ppm in the free ligand spectrum, as shown in Figure 6(a). This observation is consistent with the coordination of the carboxylic oxygen atom to the Sn center. The chemical shifts increased as the coordination number of the tin atom increased. In all complexes, the N–H proton of the ligand appeared as a singlet, confirming that the nitrogen atom does not participate in coordination with the tin center (Arraq and Hadi, 2022). All these signals shifted due to the complexity (Hadi et al., 2021). The ^{1}H-NMR spectra exhibited an exchangeable singlet in the range of 9.91–9.44 ppm, assigned to the NH proton. Several signals were observed between 8.68 and 7.61 ppm, corresponding to the aromatic protons. The methyl protons attached to the aryl ring appeared as singlets between 2.73 and 3.97 ppm. Furthermore, the methyl protons bonded to the tin atom in complex T3 appeared as a singlet at a high-field position of 0.857 ppm due to the strong shielding

effect, as shown in Figure 6(b) (Hashim et al., 2023a).

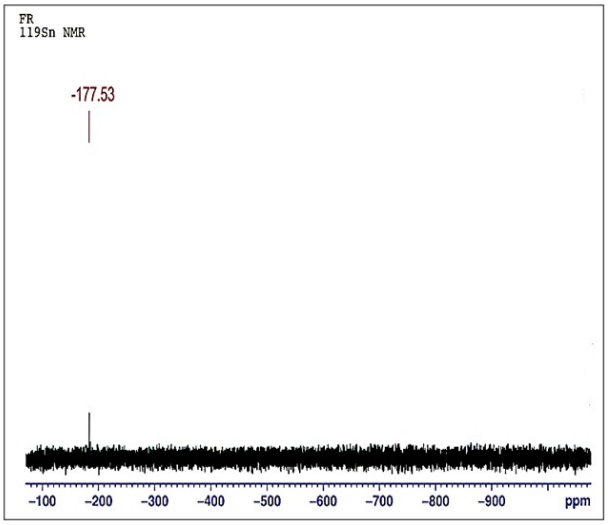

Figure 8. ^{119}Sn-NMR Spectra for the Complex T3

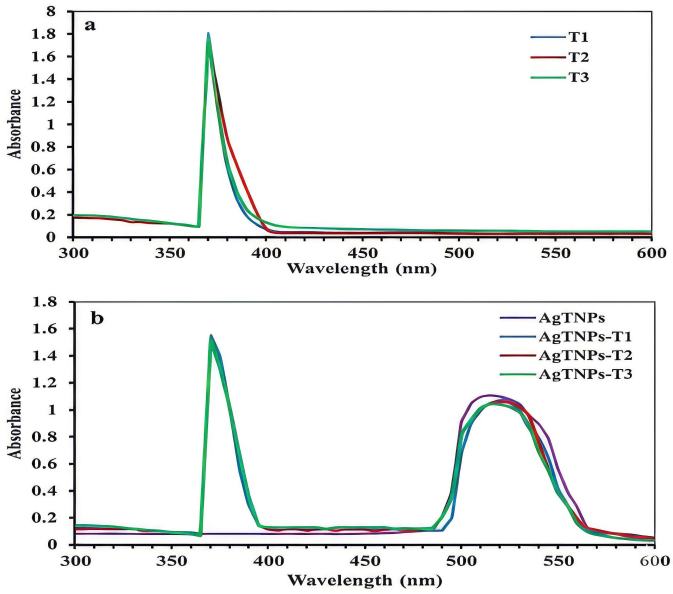

Figure 9. UV-Visible of: (a) Tri-Organotin (IV) Complexes (T1-T3), (b) Tri-Organotin (IV) Complexes (T1-T3) After Modification with AgTNPs

The ^{13}C-NMR spectra exhibited all predicted signals for the ligand and its complexes. In the spectra of complex T3, multiple signals were observed in the aromatic region. The carboxylate carbon showed a resonance at approximately 176 ppm, representing a downfield shift upon complexation, as shown in Figure 7. This deshielding effect is a direct consequence of the coordination of the carbonyl oxygen to the Sn (IV) center, which withdraws electron density from the carbon atom. The observed chemical shift values are consistent with a bidentate coordination mode, where the carboxylate group interacts strongly with the tin center, as corroborated by the FT-IR data (Al-Shemary et al., 2024). The ^{119}Sn-NMR spectra were analyzed to determine the coordination geometry of the synthesized complexes; a value less than 200 indicates five-coordinate complexes, while a value over 200 suggests six-coordinate complexes with an octahedral geometry. The complex T3 appears at (-177.53 ppm), as shown in Figure 8, which is consistent with a five-coordinate trigonal bipyramidal geometry (Malathi et al., 2022).

3.3 UV-Vis Spectrophotometry

The optical properties of the tri-organotin (IV) complexes (T1–T3) and their modified versions with triangular silver nanoparticles (AgTNPs-T1, AgTNPs-T2, and AgTNPs-T3) were examined using UV-Vis spectroscopy. As shown in Figure 9(a), the pristine tri-organotin (IV) complexes exhibited sharp absorption bands centered at approximately 370 nm, attributed to electronic transitions within the complex framework. Following modification, the UV-Vis spectra of the AgTNPs-modified complexes (AgTNPs-T1, AgTNPs-T2, and AgTNPs-T3) displayed a distinct dual-peak pattern, as illustrated in Figure 9(b). This change indicates the successful integration of the silver nanoparticles and the emergence of their characteristic surface plasmon resonance (SPR) features. A broad and prominent absorption band was observed in the range of 500-600 nm, which is a classic signature of triangular silver nanoparticles. The emergence of this band at longer wavelengths, compared to spherical nanoparticles, confirms the successful synthesis of the triangular morphology of the AgTNPs. Crucially, the coexistence of the complex-specific peaks at 370 nm with AgTNPs bands provides strong evidence for the successful loading and stabilization of the tri-organotin (IV) complexes onto the silver nanoparticle surfaces (Yin et al., 2022).

3.4 Scanning Electron Microscopy (SEM) Analysis

Scanning Electron Microscopy (SEM) analysis was employed to confirm the structural and morphological properties of the synthesized materials. The results revealed that the silver nanoparticles (AgTNPs) exhibit a distinct triangular shape with uniform dimensions and sharp edges (Abed-Al Zahra and Hadi, 2025), as described in previous research Mohsin et al. (2026). Furthermore, when these AgTNPs were used to modify the tri-organotin (IV) complexes, the SEM images revealed a significant morphological transition toward a highly uniform and porous structure. Figures 10 (b-d) show that the modified complexes (AgTNPs-T1, AgTNPs-T2, and AgTNPs-T3) possess homogeneous, porous frameworks. Additionally, the micrographs reveal the presence of small agglomerates, where the tri-organotin (IV) complexes exhibit varied morphologies and particle size distributions on the AgTNPs surfaces (Hadi et al., 2019). The particle size distribution of the AgTNPs before and after modification with tri-organotin (IV) complexes is illustrated in the following histogram. The diameters were determined using ImageJ software, as shown in Figure 11.

Table 3. Antifungal Activity For Tri-Organotin (IV) Complexes (T1-T3) with and without Modification Of AgTNPs

The Complexes	Concentration (mg/mL)	R1	R2	R3	Mean	Inhibition %	S.D	p-Value	p-Value Vs Control
Nystatin (Control)	1 mg/mL	5.2	5.15	5.2	5.18	14	0.028867	-	-
	2 mg/mL	4.5	4.45	4.5	4.48	25	0.028867	-	-
T1	1 mg/mL	5.7	5.65	5.7	5.68	5	0.028868	p < 0.001	p < 0.001
AgTNPs-T1	1 mg/mL	4.9	4.95	4.8	4.9	18	0.076376		p < 0.01
T1	2 mg/mL	5.35	5.35	5.3	5.35	11	0.028868	p < 0.001	p < 0.001
AgTNPs-T1	2 mg/mL	4.6	4.75	4.7	4.7	22	0.076376		p < 0.01
T2	1 mg/mL	5.5	5.4	5.5	5.5	8	0.057735	p < 0.001	p < 0.001
AgTNPs-T2	1 mg/mL	4.4	4.3	4.4	4.4	27	0.057735		p < 0.05
T2	2 mg/mL	5	5.11	5	5.03	16	0.063509	p < 0.001	p < 0.001
AgTNPs-T2	2 mg/mL	3.7	3.7	3.6	3.7	38	0.076376		p < 0.01
T3	1 mg/mL	5.3	5	5	5.1	15	0.173205	p < 0.001	p < 0.001
AgTNPs-T3	1 mg/mL	3.36	3.4	3.4	3.4	43	0.023094		p < 0.05
T3	2 mg/mL	4.7	4.8	4.8	4.8	20	0.057735	p < 0.001	p < 0.001
AgTNPs-T3	2 mg/mL	2.65	2.7	2.7	2.68	55	0.028868		p < 0.001

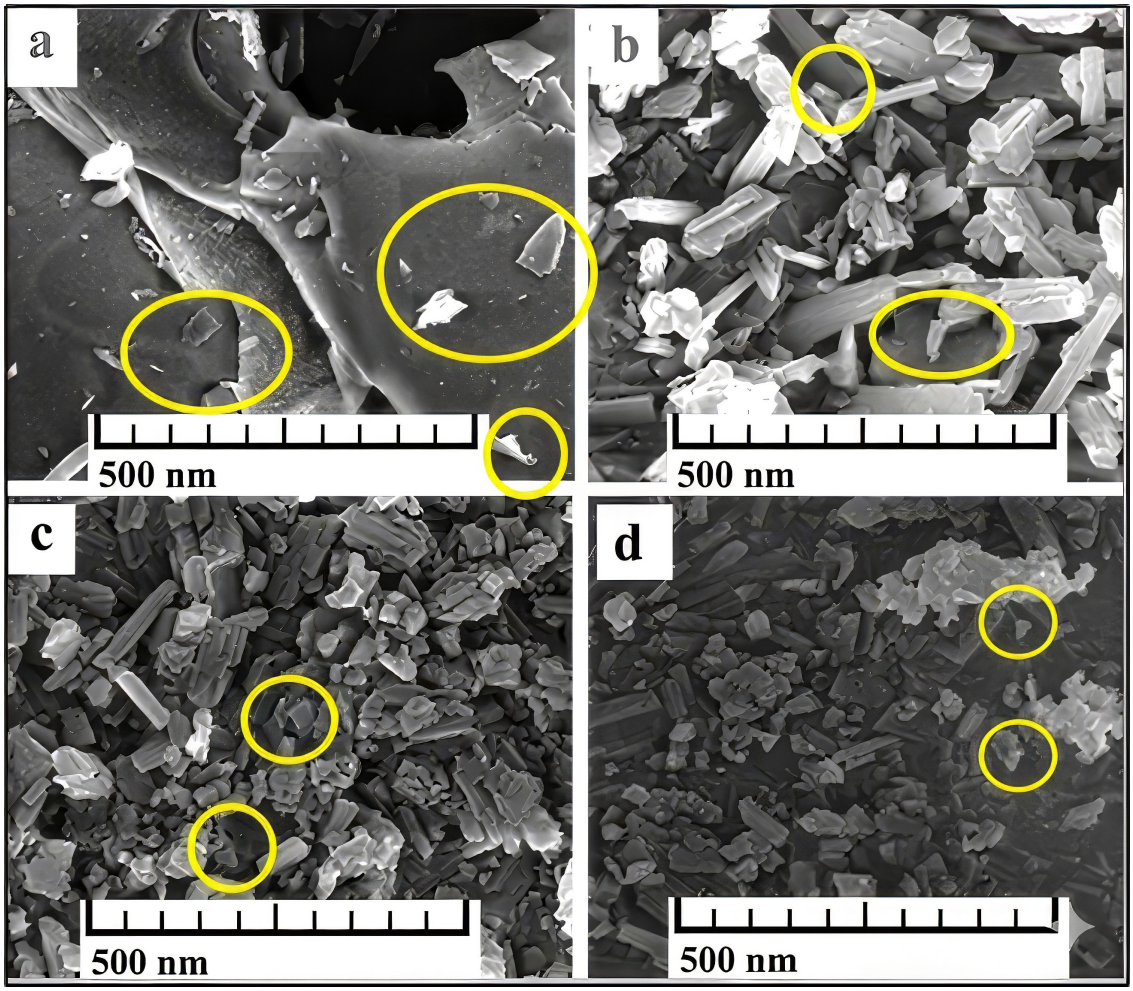

Figure 10. SEM of: (a) AgTNPs, (b) AgTNPs-T1, (c) AgTNPs-T2, (d) AgTNPs-T3

3.5 Antifungal Activity

The antifungal potential of synthesized tri-organotin (IV) complexes (T1-T3) in their original form and their modified forms with triangular silver nanoparticles (AgTNPs) was tested in vitro against *Fusarium spp*., a phytopathogenic fungus of considerable concern in the region. Figure 12 and Table 3 show the antifungal potential of synthesized complexes in their original and modified forms against *Fusarium spp*., where antifungal

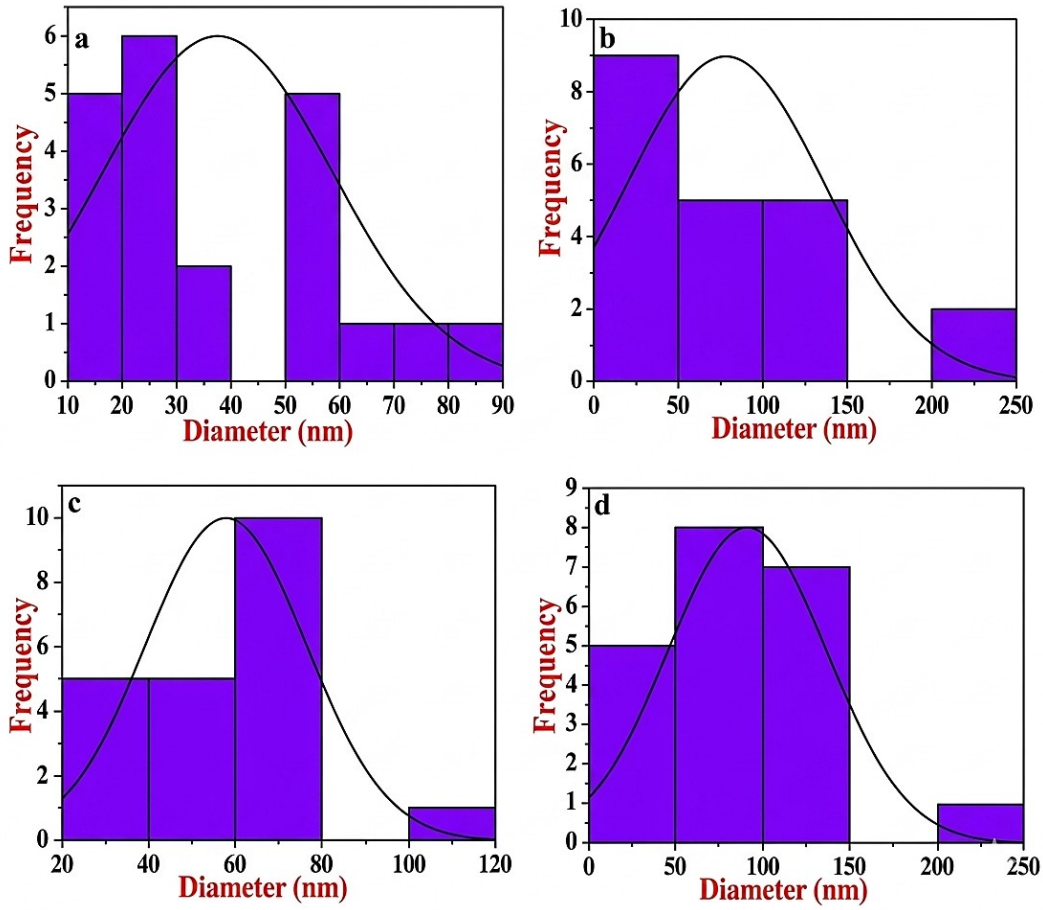

Figure 11. Particle Size Distribution Analysis of: (a) AgTNPs, (b) AgTNPs-T1, (c) AgTNPs-T2, (d) AgTNPs-T3

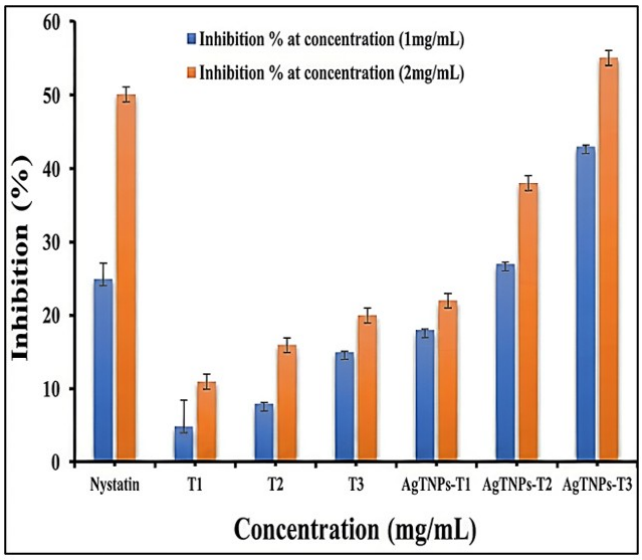

Figure 12. Inhibition Rate for Tri-Organotin (IV) Complexes Before and After Modification with AgTNPs

potential is shown in percentage inhibition of fungal growth. Literature indicates that the antifungal efficacy of tin complexes increases with their lipid solubility. This enables them to traverse the cytoplasmic membrane and thereafter serve as a potential location of action. Despite their considerable antifungal efficacy, these complexes exhibit reduced efficiency compared to the positive control (Hashim et al., 2023b). Figure 13 demonstrates that it influences the antifungal activity of the tri-organotin (IV) complexes before and after modification with AgTNPs. The tri-organotin (IV) complexes have been examined by using two concentrations (1 and 2 mg/mL). At 2 mg/mL, complex T3 showed the highest inhibition (20%) compared to T1 and T2 that it is more active mainly because the triphenyltin group in T3 is more fat-loving (lipophilic) and more aromatic than the alkyltin groups in T1 and T2, making it more easily pass through the cell membrane of the fungus and exhibited more activity than the other produced complexes, probably attributable to the presence of three phenolic groups and an elevated aromatic content relative to the other complexes (Ali et al., 2021).

On the other hand, the results of the antifungal activity after for tri-organotin (IV) complexes after modification with

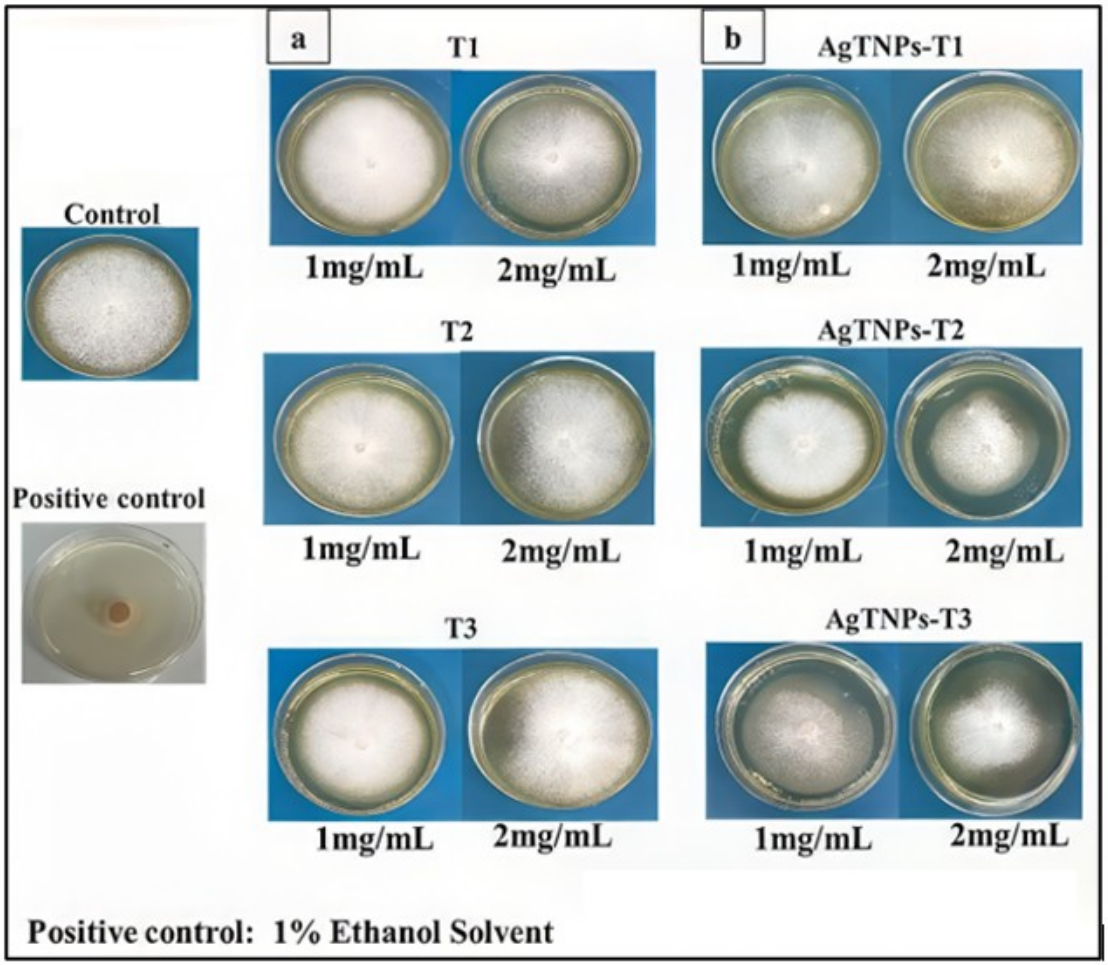

Figure 13. Antifungal Activity for: (a) Tri-Organotin (IV) Complexes (T1-T3), (b) Tri-Organotin (IV) Complexes After Modification with AgTNPs

AgTNPs significantly enhanced these results, the AgTNPs-T3 complex achieved an inhibition percentage inhibition of (55%) by AgTNPs-T3 at a concentration of 2 mg/mL, which represent a 2.75-fold higher activity compared to the unmodified complex. These findings indicate that AgTNPs modified with tri-organotin (IV) complexes exhibit improved inhibitory effects, with efficacy increasing at higher concentrations, as shown in Table 3.

Additionally, the significant improvement in the antifungal activity upon modification with AgTNPs can be explained on the basis of several synergistic factors. Firstly, the organotin complexes, particularly T3 with high aromatic constituents, are known to be poorly soluble in aqueous media. Upon conjugation with AgTNPs, which are more soluble in aqueous media, the solubility of these complexes in the aqueous medium of the test is enhanced, thereby increasing the bioavailability of these conjugates for interaction with fungal cells. Secondly, triangular silver nanoparticles are known for having sharp edges and vertices that provide a high surface area and high reactivity on the surface. These nanoparticles are likely to provide higher adhesion on the fungal cell membrane and induce physical disruption of the membrane, thereby increasing the concentration of the organotin complex at the point of action (Yin et al., 2022; Rodriguez Barroso et al., 2023). Finally, silver nanoparticles are known for their inherent antifungal activity against various fungal species through the generation of reactive oxygen species (ROS) on the fungal membrane (Han et al., 2024). The inherent antifungal activity of the organotin complex against fungal cells is known to be mediated through disruption of mitochondrial function and membrane transport processes. The combined effect of these two factors on fungal cells results in a synergistic enhancement of the conjugates' antifungal activity.

3.6 Comparative Antifungal Activity

The antifungal activity of the synthesized compounds compares well with those previously reported for the organotin (IV) systems. For instance, Joshi et al. (2020) reported the synthesis of tri-organotin (IV) complexes with a triazole-based Schiff base ligand and recorded inhibition rates of 40-60% against

Aspergillus niger and *Candida albicans* at higher concentrations (4 mg/mL). Similarly, Nopitasari et al. (2021); Dias et al. (2015) reported the synthesis of di- and tri-organotin (IV) carboxylates with antifungal activity that varied from 30-50% against Fusarium oxysporum at a concentration of 5 mg/mL. In contrast, the nano-formulated synthesized AgTNPs-T3 complex recorded an inhibition rate of 55% against *Fusarium spp*. at a substantially lower concentration of (2 mg/mL). Moreover, unlike many of the previously reported complexes that show antifungal activity only at higher concentrations of (4-5 mg/mL) (Mahdi et al., 2023; Du et al., 2011), the AgTNPs-T3 complex herein displays enhanced efficacy at a (2 mg/mL).

4. CONCLUSIONS

In conclusion, this study successfully achieved the synthesis and characterization of three novel tri-organotin (IV) complexes derived from a ciprofloxacin-based hybrid ligand, further enhanced through nano-formulation with triangular silver nanoparticles (AgTNPs). The comprehensive spectroscopic analysis, including FT-IR, NMR (^{1}HNMR, ^{13}C-NMR, and ^{119}Sn-NMR), SEM, and CHNS, confirmed the formation of stable complexes with a deformed trigonal bipyramidal geometry and highlighted the successful integration of the organotin moieties onto the porous surface of the triangular nanostructures. Biological evaluation against *Fusarium spp*. demonstrated a remarkable synergistic effect, where the nano-formulated conjugates, particularly the triphenyltin derivative (AgTNPs-T3), exhibited superior antifungal efficacy at significantly lower concentrations compared to both the pure complexes and previously reported organotin systems. These findings suggest that the combination of the membrane-disrupting properties of AgTNPs and the mitochondrial interference of tri-organotin (IV) complexes provides a potent strategy for developing next-generation antifungal agents. Ultimately, this research underscores the potential of nano-enhanced organometallic compounds as efficient, low-dosage alternatives for controlling resistant fungal pathogens in both medicinal and agricultural applications.

5. ACKNOWLEDGEMENT

The University of Babylon, College of Science, Department of Chemistry all are thanked for financial support.

REFERENCES

Abed-Al Zahra, M. A. A. and A. G. Hadi (2025). Synthesis, Characterization, and Antioxidant Activity of Novel Diorganotin(IV) Complexes Derived from Ibuprofen-5-Aminosalicylic Acid Ligand. *Journal of Kufa for Chemical Sciences*, **39**(1); 1–23

Al-Refaia, R. A. K., L. Ahmed, A. A. Alkarimi, S. S. Al-Obaidy, F. A. Hussein, and D. N. Taha (2019). New Approaches for Preparation of Silver Nanoparticles Using Quince Plant Extract as Antibacterial Agents. *Journal of Global Pharma Technology*, **11**(9); 140–143

Al-Refaia, R. A. K., E. Alrikabi, A. A. Alkarimi, and R. Vasiliadou (2024). A New Synthesis of Copper Nanoparticles and Its Application as a Beta-Hematin Inhibitor. *Indonesian Journal of Chemistry*, **24**(1); 152–159

Al-Shemary, R. S., H. Jasem, A. G. Hadi, and S. J. Baqir (2024). Boosted Antibacterial Efficacy: Di and Triorganotin Complexes via 2-[(2,3-Dimethylphenyl)Amino] Benzoic Acid. *Bulletin of the Chemical Society of Ethiopia*, **38**(3); 647–655

Ali, A. R., H. A. A. Anani, and F. M. Selim (2021). Biologically Formed Silver Nanoparticles and In Vitro Study of Their Antimicrobial Activities on Resistant Pathogens. *Iranian Journal of Microbiology*, **13**(6); 848–861

Ali, S. A. R., R. A. Al Refaia, E. Alrikabi, K. O. Ali, A. N. Hussein, A. A. Alkarimi, and A. R. Al Shujairi (2025). Synthesis, Characterization of Silver Nanoparticles Using Rosemary Extract and Their Application as Antioxidant, Antifungal and Antibacterial Agents. *Journal of Nanostructures*, **15**(3); 885–895

Arraq, R. R. and A. G. Hadi (2022). Enhanced the Antioxidant Activity of Tri Organotin (IV) Complexes Derived from Cephalexin. *Azerbaijan Medical Journal*, **62**(06); 2197–2209

Chandrakala, V., V. Aruna, and G. Angajala (2022). Review on Metal Nanoparticles as Nanocarriers: Current Challenges and Perspectives in Drug Delivery Systems. *Emergent Materials*, **5**(6); 1593–1615

Dias, L. C., G. M. De Lima, J. A. Takahashi, and J. D. Ardisson (2015). New Di- and Triorganotin (IV) Carboxylates Derived from a Schiff Base: Synthesis, Characterization and In Vitro Antimicrobial Activities. *Applied Organometallic Chemistry*, **29**(5); 305–313

Du, D., Z. Jiang, C. Liu, A. M. Sakho, D. Zhu, and L. Xu (2011). Macrocyclic Organotin (IV) Carboxylates Based on Benzenedicarboxylic Acid Derivatives: Syntheses, Crystal Structures and Antitumor Activities. *Journal of Organometallic Chemistry*, **696**(13); 2549–2558

Erfan, A., E. Yousif, A. Alshanon, and G. El-Hiti (2024). Organotin(IV) Complexes as Chemotherapeutic Drugs Against Different Types of Cancer Cell Lines: A Review. *Al-Nahrain Journal of Science*, **27**(5); 70–77

Fithri, N. A., A. Fadilah, A. Pratiwi, S. S. Alisyahbana, M. F. Alhafiz, and N. Puan (2025). *Uncaria gambir* Based Green Synthesis of Inorganic Nanoparticles for Photothermal Induced Thrombolytic and Antibacterial Applications. *Science and Technology Indonesia*, **10**(1); 1–15

Hadi, A. G., S. J. Baqir, D. S. Ahmed, G. A. El-Hiti, H. Hashim, A. Ahmed, B. M. Kariuki, and E. Yousif (2021). Substituted Organotin Complexes of 4-Methoxybenzoic Acid for Reduction of Poly(Vinyl Chloride) Photodegradation. *Polymers*, **13**(22); 1–17

Hadi, A. G., K. Jawad, E. Yousif, and G. A. El-Hiti (2019). Synthesis of Telmisartan Organotin(IV) Complexes and Their Use as CO_2 Capture Media. *Molecules*, **24**(8); 1631

Han, M., Z. Xia, Y. Zou, P. Hu, M. Zhang, X. Yang, M. G. Ma, and R. Yang (2024). Comparative Study and Transcriptomic

Analysis on the Antifungal Mechanism of Ag Nanoparticles and Nanowires Against *Trichosporon asahii*. *International Journal of Nanomedicine*, **19**; 11789–11804

Hano, C. and B. H. Abbasi (2022). Plant-Based Green Synthesis of Nanoparticles: Production, Characterization and Applications. *Biomolecules*, **12**(1); 1–9

Hashim, D. J., E. H. Al-Rikabi, A. G. Hadi, and S. J. Baqir (2023a). 4-Aminoantipyrine-New Organotin Complexes, Synthesis, Structure and Antioxidant Activity. *Bulletin of the Chemical Society of Ethiopia*, **37**(5); 1163–1170

Hashim, D. J., E. J. Waheed, A. G. Hadi, and S. J. Baqir (2023b). Exploring the Biological Activity of Organotin Carboxylate Complexes with 4-Sulfosalicylic Acid. *Bulletin of the Chemical Society of Ethiopia*, **37**(6); 1–23

Joshi, R., A. Kumari, K. Singh, H. Mishra, and S. Pokharia (2020). Triorganotin(IV) Complexes of Schiff Base Derived from 1,2,4-Triazole Moiety: Synthesis, Spectroscopic Investigation, DFT Studies, Antifungal Activity and Molecular Docking Studies. *Journal of Molecular Structure*, **1206**; 127639

Li, N., J. Ma, X. Du, Y. Shi, P. Zhao, Q. Li, and C. Ma (2025). Syntheses, Structures, In Vitro Cytostatic Activity and Antifungal Activity Evaluation of Six Organotin(IV) Complexes Based on Quinoline-6-Carboxylic Acid. *Journal of Organometallic Chemistry*, **1035**; 123685

Mahdi, I. J., N. S. Saddam, A. G. Hadi, S. J. Baqir, Y. F. Al-Khafaji, and A. S. Abbas (2023). Identification and Antioxidant Activity of Di and Tri-Organotin Complexes Derived from Cinnamic Acid. *Egyptian Journal of Chemistry*, **66**(4); 213–218

Malathi, S., D. Manikandan, R. Nishanthi, E. G. Jagan, S. U. M. Riyaz, P. Palani, and J. Simal-Gandara (2022). Silver Nanoparticles, Synthesized Using *Hyptis suaveolens* (L.) Poit and Their Antifungal Activity Against *Candida* spp. *ChemistrySelect*, **7**(47); e202203050

Mohsin, A. D., R. A. K. Al-Refaia, and A. G. Hadi (2026). Green Synthesis of Triangular Silver Nanoparticles Using Garden Cress Seed Extract Based on Gallic Acid and Their Antifungal Activity. *Journal of Nanostructures*, **16**(1); 474–483

Nopitasari, T., T. Suhartati, S. Suharso, D. Herasari, K. D. Pandiangan, and S. Hadi (2021). Synthesis, Characterization, and Antioxidant Activity of Some Organotin(IV) 2-Nitrobenzoate Using the 2,2-Diphenyl-1-Picryl-Hydrazyl (DPPH) Method. *Journal of Physics: Conference Series*, **1751**(1); 012098

Polinarski, M. A., A. L. B. Beal, F. E. B. Silva, J. Bernardi-Wenzel, G. R. M. Burin, G. I. B. de Muniz, and H. J. Alves (2021). New Perspectives of Using Chitosan, Silver, and Chitosan–Silver Nanoparticles Against Multidrug-Resistant Bacteria. *Particle & Particle Systems Characterization*, **38**(4); 2100009

Preethi, A. C., V. Hariharakrishnan, and V. Saraswathi (2024). The Optical and Electrochemical Characteristics of Silver Nanoparticles, Besides Antibacterial and Antifungal Properties Using *Crocus sativus* L. Petal. *Journal of Optoelectronic and Biomedical Materials*, **16**(4); 199–209

Qiao, W., Y. Liu, X. Fan, Y. Yang, W. Liu, L. Wang, and Z. Hu (2023). Rapid and Sensitive Determination of Ascorbic Acid Based on Label-Free Silver Triangular Nanoplates. *Current Research in Food Science*, **7**; 100548

Radulescu, D. M., V. A. Surdu, A. Ficai, D. Ficai, A. M. Grumezescu, and E. Andronescu (2023). Green Synthesis of Metal and Metal Oxide Nanoparticles: A Review of the Principles and Biomedical Applications. *International Journal of Molecular Sciences*, **24**(20); 15397

Raji, S. Q. and A. T. Bader (2024). Synthesis and Characterization of Ni^{2+} Schiff Base Complex as a Precursor for NiO Nanoparticles and an Investigation of Their Corrosion Inhibition. *Science and Technology Indonesia*, **9**(4); 914–928

Rodriguez Barroso, L. G., E. L. Garcia, M. Mojicevic, M. Huerta, R. Pogue, D. M. Devine, and M. Brennan-Fournet (2023). Triangular Silver Nanoparticles Synthesis: Investigating Potential Application in Materials and Biosensing. *Applied Sciences*, **13**(14); 8100

Saputra, K., M. Masruroh, H. Susanto, and R. Apsari (2024). Tapping into the Power of Sol-Gel Method for Enhanced Antimicrobial Activity of Titania Nanoparticles. *Science and Technology Indonesia*, **9**(3); 546–555

Soleimani, P., A. Mehrvar, J. P. Michaud, and N. Vaez (2022). Optimization of Silver Nanoparticle Biosynthesis by Entomopathogenic Fungi and Assays of Their Antimicrobial and Antifungal Properties. *Journal of Invertebrate Pathology*, **190**; 107749

Yin, M., X. Xu, H. Han, J. Dai, R. Sun, L. Yang, J. Xie, and Y. Wang (2022). Preparation of Triangular Silver Nanoparticles and Their Biological Effects in the Treatment of Ovarian Cancer. *Journal of Ovarian Research*, **15**(1); 1–14

